Lipophilic tetraphenylphosphonium derivatives enhance radiation-induced cell killing via inhibition of mitochondrial energy metabolism in tumor cells

Hironobu Yasui[a,b,$], Kumiko Yamamoto[a,$], Motofumi Suzuki[a], Yuri Sakai[a], Tomoki Bo[a], Masaki Nagane[a], Eri Nishimura[a], Tohru Yamamori[a], Toshihide Yamasaki[c, 1], Ken-ichi Yamada[c, d], Osamu Inanami[a*]

[a] Laboratory of Radiation Biology, Department of Environmental Veterinary Sciences, Graduate School of Veterinary Medicine, Hokkaido University, Sapporo 060-0818, Japan

[b] Central Institute of Isotope Science, Hokkaido University, Sapporo 060-0815, Japan

[c] Physical Chemistry for Life Science Laboratory, Faculty of Pharmaceutical Sciences, Kyushu University, Fukuoka 812-8582, Japan

[d] Japan Science and Technology Agency, PRESTO, 4-1-8 Honcho, Kawaguchi, Saitama 332-0012, Japan

[$] These authors contributed to this work equally.

[1] Present Address: Aix-Marseille Université, Institut de Chimie Radicalaire, Case 551 - Campus St Jérôme, Avenue Escadrille Normandie Niemen, 13397 Marseille, Cedex 20, France

*Corresponding Author

Address: Kita 18, Nishi 9, Kita-ku, Sapporo, Hokkaido 060-0818, Japan.

Tel.: +81 11 706 5235, Fax: +81 11 706 7373

Email: inanami@vetmed.hokudai.ac.jp

Abstract

It has recently been reported that radiation enhances mitochondrial energy metabolism in various tumor cell lines. To examine how this radiation-induced alteration in mitochondrial function influences tumor cell viability, various lipophilic triphenylphosphonium (TPP^+) cation derivatives and related compounds such as 4-hydroxy-2,2,6,6-tetramethyl-1-oxy-piperidin (Tempol) with TPP^+ (named "Mito-") were designed to inhibit the mitochondrial electron transport chain. Mito-$(CH_2)_{10}$-Tempol (M10T) and its derivatives, Mito-$(CH_2)_5$-Tempol (M5T), Mito-$(CH_2)_{10}$-Tempol-Methyl (M10T-Me), Mito-$C_{10}H_{21}$ (M10), and $C_{10}H_{21}$-Tempol (10T), were prepared. In HeLa human cervical adenocarcinoma cells and A549 human lung carcinoma cells, the fractional uptake of the compound into mitochondria was highest among the TTP^+ analogs conjugated with Tempol (M10T, M5T, and 10T). M10T, M10T-Me, and M10 exhibited strong cytotoxicity and enhanced X-irradiation-induced reproductive cell death, while 10T and M5T did not. Furthermore, M10T, M10T-Me, and M10 decreased basal mitochondrial membrane potential and intracellular ATP. M10T treatment inhibited X-ray-induced increases in ATP production. These results indicate that the TPP cation and a long hydrocarbon linker are essential for radiosensitization of tumor cells. The reduction in intracellular ATP by lipophilic TPP^+ is partly responsible for the observed radiosensitization.

Keywords

ATP, Cancer, Mitochondria, Radiation, Reactive oxygen species, Triphenylphosphonium

1. Introduction

Unlike normal cells, most cancer cells generate energy by converting glucose to lactate even in the presence of oxygen, a unique metabolic feature called aerobic glycolysis. Consequently, the majority of glycolysis-derived pyruvate in cancer cells is believed to be diverted to lactate fermentation and kept away from mitochondrial oxidative metabolism. Despite this well-known metabolic phenotype of cancer cells (referred to as the Warburg effect [1]), many cancer cells retain non-negligible mitochondrial functions. These functions include respiration, ATP generation, reactive oxygen species (ROS) production, apoptosis induction, calcium regulation, and redox regulation. These mitochondrial functions in cancer cells are associated with not only cell energy homeostasis but also carcinogenesis, cell death, and metastasis [2, 3].

Accumulating evidence suggests that agents of genotoxic damage, including ionizing radiation (IR) alter mitochondrial structure and functions (mass, morphology, respiration, and ROS production) in cancer cells [4-6]. Our previous report demonstrated that the rotenone-sensitive oxygen consumption rate (OCR) increased 12–24 h after irradiation in various reproductive cancer cell lines (i.e., human lung carcinoma A549 cells, human cervical carcinoma HeLa cells, human gastric cancer MKN45 cells, human melanoma MeWo cells, and mouse fibroblast NIH3T3 cells) [7]. It has also been reported that radiation-induced G2/M arrest contributes to increased mitochondrial membrane potential, production of mitochondria-derived ATP, ROS production, and mitochondrial fission [7, 8]. On the other hand, Lu *et al.* have demonstrated that mTOR signaling plays a key role in this switching process from glycolysis to oxidative phosphorylation in energy metabolism [9]. This radiation-induced switching process in energy metabolism may be an adaptive response

to genotoxic damage (apoptosis, cell cycle checkpoint activation, and DNA damage repair) [10]. However, no experimental evidence suggests that this increase in ATP is essential for survival of tumor cells. If the radiation-induced activation of mitochondrial function is indispensable to irradiated tumor cell survival, specific and moderately inhibitory reagents targeting the mitochondrial electron transport chain (ETC) might enhance the tumor cell cytotoxicity of radiation therapy.

Triphenylphosphonium (TPP^+) conjugated with biologically active small molecules such as thiol probes [11, 12], spin-traps [13-15], superoxide probes [16], and antioxidants [17-19] have been developed to modify mitochondrial function against various oxidative stresses, as summarized by Murphy *et al*. [20]. Recently, more hydrophobic longer alkyl chain TPP^+ derivatives, i.e., decyl TPP^+ ($C_{10}TPP^+$) and dodecyl TPP^+ ($C_{12}TPP^+$), were reported to inhibit oxidative phosphorylation in mitochondria irrespective of the characteristics of the conjugated active small molecules. Trendeleva *et al.* revealed that micro-molar concentrations of $C_{12}TPP^+$ inhibited state 3 respiration, decreased mitochondrial membrane potential, and potentiated the uncoupling effect of fatty acids, leading to mitochondrial swelling [21, 22]. Furthermore, $C_{10}TPP^+$ and $C_{12}TPP^+$ were shown to increase proton leakage, decrease maximal respiration, and inhibit the activities of complex I and III [23]. Treatment with Mito-Q (coenzyme-Q conjugated to a $C_{10}TPP^+$) and Mito-CP (a 5-membered nitroxide, CP, conjugated to a $C_{11}TPP^+$) in the presence of 2-deoxyglucose were also reported to potently inhibit cellular ATP generation and enhance cell death in human breast cancer MCF-7 cells, despite these TPP^+ compounds possessing anti-oxidative activity [21]. These findings indicate that the longer alkyl chain TPP^+ derivatives effectively inhibit mitochondrial oxidative phosphorylation.

In the present study, a series of lipophilic TPP^+ derivatives and related compounds shown in Figure 1A (TPP^+, named "Mito-"); Mito-$(CH_2)_{10}$-Tempol (M10T), Mito-$(CH_2)_5$-Tempol (M5T), Mito-$(CH_2)_{10}$-Tempol-Methyl (M10T-Me), $C_{10}H_{21}$-Tempol (10T), and (1-decyl) triphenylphosphonium bromide (M10), were newly synthesized. The relationship between the structures of these compounds and their effects on mitochondrial membrane potential and ROS production were evaluated in HeLa cells and A549 cells. To clarify how radiation-induced increases in mitochondrial energy metabolism influence tumor cell viability, the effects of sub-lethal doses of these lipophilic TPP^+ derivatives on colony-forming ability of tumor cells exposed to X-rays were examined.

2. Materials and Methods

2.1 Reagents

M10T, M5T, M10T-Me, and 10T were synthesized as described in supplemental information. M10 was purchased from Santa Cruz Biotechnology (Dallas, TX, USA). Other reagents without specific descriptions were obtained from Wako Pure Chemical Industries (Osaka, Japan). The following antibodies were used for immunoblotting: anti-Lamin B (Calbiochem/Merck Millipore, Darmstadt, Germany), anti–voltage-dependent anion-selective channel protein 1 (VDAC1), anti–glyceraldehyde 3-phosphate dehydrogenase (GAPDH), and horseradish peroxidase (HRP)-conjugated secondary antibodies (Santa Cruz Biotechnology).

2.2 Cell culture

Human cervical adenocarcinoma cells (HeLa) and human lung carcinoma cells (A549) were purchased from the RIKEN Cell Bank. These cell lines are widely used in analyses of radiosensitivity due to their high plating efficiency and stable radioresponse [24-26]. Cells were grown in D-MEM medium (Gibco-BRL/Thermo Fisher Scientific Co., Carlsbad, CA, USA) and RPMI 1640 medium (Gibco-BRL/Thermo Fisher Scientific Co.), respectively. Both media were supplemented with 10 % fetal bovine serum (FBS: Biowest, Nuaille, France). Cells were maintained at 37°C in 5% CO_2 / 95 % air.

2.3 X-irradiation and reagent treatment

Cells in 60 mm or 90 mm plastic dishes were allowed to adhere, and then treated with M10T, 10T, M5T, M10T-Me, or M10 at the indicated concentrations for 12 h. Treatment time was set at roughly one half of the doubling time (24 h for HeLa, 22 h for A549) to minimize the influence of cell cycle-dependent increases or decreases in mitochondria. In studies combining compound treatment with X-irradiation, cells were exposed to X-rays after compounds were removed by replacement with fresh medium. Irradiation (IR) was performed using an X-RAD iR-225 (1.0 mm Al filter, 200 kVp, 15 mA; Precision X-ray, North Brandford, CT, USA).

2.4 Clonogenic survival assay

Appropriate numbers of tumor cells were treated with compounds and/or IR. After treatment, HeLa and A549 cells were cultured for eight and ten days, respectively. Cell colonies were fixed, stained with Giemsa stain, and scored under a microscope. Only colonies containing > 50 cells were scored as surviving cells. After the surviving

fraction at each dose was calculated with respect to the plating efficiency of the non-irradiated control, the mean ± standard deviation (S.D.) of the surviving fractions obtained from three experiments was plotted. The survival curves were fitted to a linear-quadratic (LQ) model: SF = exp $(-\alpha D - \beta D^2)$, where SF is the surviving fraction and D is the physical dose, by data analysis software Origin Pro 7 (OriginLab Co., Northampton, MA, USA).

2.5 Detection of nitroxide in mitochondria by electron spin resonance (ESR) spectroscopy

Isolation of intact mitochondria was performed according to the method of Trounce et al.[27] with some modifications. Briefly, the suspension of HeLa cells (1×10^7 cells) was treated with 10 μM M10T, M5T, or 10T for 30 min at 37 °C. After twice washing with PBS(-), cells were resuspended in ice-cold isolation buffer (2.5 mM Hepes-KOH, pH 7.4, 70 mM sucrose, 220 mM mannitol, 1 mM EGTA). This was followed by repeated passages through a glass-Teflon Potter-Elvehjem pestle and glass tube. Nuclei and debris were collected by centrifuging the suspension twice at 1000 g for 10 min at 4°C, and resuspending in 100 μL lysis buffer (50 mM Tris-HCl, pH 7.5, 1% [vol/vol] Triton X-100, 5% [vol/vol] glycerol, 5 mM EDTA, and 150 mM NaCl). The supernatant was further centrifuged twice at 10000 g for 10 min at 4°C, and the obtained pellet was resuspended in 100 μL of lysis buffer. This resuspension was the mitochondrial fraction. Final supernatants (1.8 mL) were collected and represent cytoplasmic fractions, diluted to one-eighteenth of the relative concentrations of the nuclear and mitochondrial fractions. The protein concentration in each subcellular fraction was determined using the Bio-Rad protein assay (Bio-Rad, Hercules, CA,

USA). To confirm the purity of each cell fraction, immunoblot analysis for specific markers of each fraction was performed, as described in our previous study [8].

Spin probe content in each fraction was determined by oxidation of the sample with 2 mM $K_3Fe(CN)_6$ to convert cyclic hydroxylamines into nitroxides, which can be detected by ESR. Briefly, 70 µL of each fractionated suspension was mixed with 56 µL of acetonitrile after a 5 min incubation with 14 µL of $K_3Fe(CN)_6$. One hundred and ten microliters of the oxidized sample was loaded into a quartz flat cell (Radical Research, Tokyo, Japan) and ESR spectra of nitroxide radicals were recorded using a JEOL-RE X-band spectrometer (JEOL, Tokyo, Japan) under the following conditions: incident microwave power, 5 mW; receiver gain, 100; microwave frequency, 9.1 GHz; field modulation amplitude, 79 µT; scan range, ± 7.5 mT.

2.6 Measurements of mitochondrial membrane potential and mitochondrial ROS

Tetramethylrhodamine methyl ester (TMRM, Thermo Fisher Scientific Co.) and MitoSOX red (MSR, Thermo Fisher Scientific Co.) were used as fluorescent probes for mitochondrial membrane potential and for mitochondria-derived ROS, respectively [28]. Exponentially growing HeLa cells in 60 mm dishes were treated with 1.5 µM of each compound and/or 10 Gy of IR. At predetermined times after treatment, cells were trypsinized and washed twice with ice-cold PBS(-). Cells were then incubated in serum-free medium containing 20 nM TMRM or 5 µM MSR for 30 min at 37°C. After resuspension in PBS(-), cells were analyzed using an EPICS XL flow cytometer (Beckman Coulter, Fullerton, CA, USA). The mean fluorescence intensity of each sample was normalized to that of a control sample to calculate relative fluorescence intensity.

2.7 ATP measurement

After IR and/or treatment with compound, adherent cells were collected from 6-well plates by trypsinization, and cell suspensions were prepared at 1.25×10^5 cells/ml. For measurement of cellular ATP, a luciferin-luciferase ATP assay system (Toyo-ink, Tokyo, Japan) was used, according to protocols provided by the manufacturer.

2.8 Statistical analysis

All results were expressed as means ± S.D. The variance ratio was estimated using the F-test, and differences in group means were determined using Student's t-test or Welch's t-test. In some experiments, we performed one-factor analysis of variance (ANOVA) and subsequent Dunnett's test. The minimum level of significance was set at $p < 0.05$.

3. Results

3.1 Compounds with TPP^+ and alkyl chains of 10 carbons exhibited relatively high toxicity

To test the toxicity of lipophilic TPP^+ derivatives and their related compounds, we first performed a clonogenic survival assay for integrated evaluation of multiple forms of cell death, including apoptosis, necrosis, and mitotic catastrophe. The effect of 12-h continuous exposure to escalating concentrations of M10T, M10, M10T-Me, 10T, and M5T on the clonogenic ability of HeLa and A549 cell lines was examined. The results displayed in Fig. 1B and Table 1 reveal potent cytotoxicity with M10T, M10, and M10T-Me, whose structures contain TPP^+ and 10 alkyl chains, and their IC_{50} values were in the sub-micromolar range for both cell lines. The structurally identical analogs of 10T that lack the TPP^+ moiety, and M5T with its 5 alkyl chain did not produce cytotoxicity, suggesting that the TPP^+ moiety, and the long alkyl chain are essential for cytotoxicity. Based on these data, we used 1.5 μM for HeLa cells and 0.5 μM for A549 cells, as sublethal doses of M10T, in subsequent experiments. Cell survival after HeLa or A549 cell treatment with these respective concentrations of M10T were 80 % or greater.

3.2 Compounds with 10-carbon alkyl chains decreased mitochondrial membrane potential and increased ROS from mitochondria

We next evaluated mitochondrial membrane potential after treatment with lipophilic TPP^+ derivatives or related compounds using the fluorescent probe TMRM and a flow cytometer. As shown in Fig. 2A, treatment with M10T, M10, and M10T-Me for 12 h remarkably depolarized the mitochondrial membrane, while treatment with

M5T was much less effective. Because 10T also significantly decreased mitochondrial membrane potential, the long, 10-carbon alkyl chain structure appears to be responsible for depolarizing the mitochondrial membrane.

To investigate the possibility that mitochondrial dysfunction caused by lipophilic TPP^+ derivatives increases ROS, we quantitated cellular mitochondrial ROS using an MSR-based flow cytometric method. M10T, M10, and M10T-Me, in addition to depolarizing the mitochondrial membrane, were found to increase mitochondria-derived ROS, indicating that ROS leakage from mitochondria accompanied lipophilic TPP^+-induced mitochondrial dysfunction (Fig. 2B).

3.3 M10T accumulates in the mitochondria with high efficiency

Next, in HeLa cells, we assessed the sub-cellular distribution of M10T, M5T, and 10T, whose structures contain nitroxyl radicals, using ESR spectroscopy. After treatment with these compounds, subcellular components were fractionated. Purity of fractions was confirmed by western blot for specific markers (Fig. 3A). Mitochondrial, nuclear, and cytoplasmic fractions were analyzed by ESR. Figure 3B shows representative ESR spectra of mitochondrial and nuclear fractions derived from 5.5×10^6 cells, and cytoplasmic fraction derived from 0.31×10^6 cells. While triplet ESR signals due to nitroxide radicals were observed in all fractions from cells treated with M10T, M5T, and 10T, their signal intensities were quite different from each other. Quantitative data in which cell numbers have been adjusted to 1×10^7 and normalized to the mitochondrial fraction of M10T-treated cells are shown in Fig. 3C. While all tested compounds show significantly higher uptake into mitochondria than into nuclei, the uptake of M10T into the mitochondrial fraction was much higher than that of M5T,

which has shorter alkyl chains, and that of 10T, which does not contain TPP^+. These results suggest that both the long-alkyl chains and the TPP^+ moiety are required for high uptake into mitochondria.

3.4 Compounds with TPP^+ and 10-carbon alkyl chains demonstrated radiosensitizing activity

We next tested the radiosensitizing effects of these compounds at sublethal concentrations (determined with data in Fig. 1B). In both HeLa and A549 cells, treatment with M10T, M10, and M10T-Me, but not 10T or M5T, decreased survival after IR (Fig. 4). Table 2 lists biological parameters calculated from survival curves, and indicates that pretreatment with M10T suppresses clonogenic cell survival. Treatment with 1.5 μM M10T reduced the 10% lethal dose (D_{10}) of the surviving fraction in HeLa cells from 6.53 Gy to 4.58 Gy. The sensitizer enhancement ratio (SER), as measured by D_{10} was 1.43, indicating the increase in radiosensitivity induced by M10T. Similarly, M10 and M10T-Me enhanced IR-induced reproductive cell death, and SER values for these compounds were 1.35 and 1.37, respectively. By contrast, 10T and M5T did not exert a radiosensitizing effect, and SER values were 1.02 and 1.05, respectively. From the point of view of LQ theory, SERα was 2.18 for M10T, 2.00 for M10, and 2.13 for M10T-Me, respectively. In contrast, M10T, M10, and M10T-Me did not affect the β values. This tendency was also observed in A549 cells. These results indicate that TPP^+ and long alkyl chains are essential for enhancing radiation-induced cell killing.

3.5 M10T inhibited IR-induced ATP production, but did not influence the effect of IR on mitochondrial membrane potential and the production of ROS from mitochondria

To decipher the mechanism of radiosensitization by the lipophilic TPP^+ derivative M10T, the combined effects of M10T and IR on mitochondrial membrane potential, mitochondrial ROS levels, and ATP production were examined. As shown in Fig. 5A, 10 Gy of IR alone increased the mitochondrial membrane potential approximately 1.5 fold in HeLa cells, in agreement with our recent experiment using A549 cells [7]. Pretreatment with M10T did not significantly affect IR-induced increase in mitochondrial membrane potential, while M10T alone decreased it. Likewise, IR significantly increased ROS from mitochondria by approximately 1.5 fold. Treatment with M10T alone significantly increased the ROS level by approximately 4.5 fold. Intriguingly, there is no significant difference between the M10T group and the combination group (Fig. 5B). As shown in Fig. 6, a luminescent ATP assay demonstrated that IR significantly upregulated ATP production in HeLa cells in accord with our previous report on A549 cells [7]. Intriguingly, combination treatment with M10T completely abrogated the IR-induced increase in ATP production. This tendency was also observed in M10T-Me- and M10-treated cells. On the other hand, 10T and M5T, which did not induce radiosensitization, had no influence on basal ATP levels or the increment amount by X-irradiation on ATP levels. These results suggest that M10T inhibits cellular ATP production in response to IR, leading to radiosensitization.

4. Discussion

In this report, sub-lethal concentrations of TPP^+ derivatives with lipophilic long alkyl chains such as M10T, M10, and M10T-Me, were proven to inhibit the mitochondrial ETC. Trnka *et al.* have reported that hydrophobic TPP^+ derivatives with a long alkyl chain, i.e., decyl TPP^+ ($C_{10}TPP^+$) and dodecyl TPP^+ ($C_{12}TPP^+$), inhibit oxidative phosphorylation in mitochondria by interfering with complex I and III, irrespective of the characteristics of the conjugated active small molecule, though propyl TPP^+ (C_3 TPP^+) and heptyl TPP^+ (C_7 TPP^+) exert minor inhibitory effects. Furthermore, $C_{10}TPP^+$ and $C_{12}TPP^+$ were shown to reduce mitochondrial membrane potential by inhibiting complex I and III [23]. As shown in Fig. 1B, sub-lethal concentrations of M10T, M10T-Me, and M10 are 1.5 μM and 0.5 μM for HeLa and A549 cells, respectively. In addition, mitochondrial membrane potential in HeLa cells was strongly depressed not only in the presence of sub-lethal doses of M10 and M10T-Me, but also M10T, even though tempol is known to be a strong antioxidant. Moreover, production of ROS from mitochondria was increased by treatment with M10, M10T-Me, and M10T, as shown in Fig. 2B. These findings indicate that lipophilic decyl TPP^+ compounds inhibit oxidative phosphorylation in mitochondria irrespective of characteristics of the conjugated small molecule. Furthermore, M5T and 10T induced little decrease in mitochondrial membrane potential, and the accumulation of M5T and 10T in mitochondria was small in comparison with that of M10T, as revealed by ESR detection in Fig. 3. These observations indicate that a longer lipophilic alkyl chain and TPP^+ are necessary to inhibit ETC function and accumulate in the mitochondria. The lipid composition of the mitochondrial membrane controls its fluidity, and membrane potential, and thereby regulates cell death [29], and exogenous long chain free fatty

acids (FFA) are reported to interfere with complex I and III in mitochondrial ETC [30]. The mechanism of ETC inhibition by longer lipophilic alkyl chains in TPP^+ is unclear, but incorporation of lipophilic long alkyl chains into the mitochondria inner membrane may play a key role.

Treatment with sub-lethal concentrations of M10T, M10T-Me, and M10 induced radiosensitization in HeLa cells and A549 cells (Fig. 4), whereas inhibition of the ETC abrogated radiation-induced increases in ATP concentration and OCR (Fig. 6 and supplemental Fig. 1), but not the mitochondrial membrane potential (Fig. 5A). Moreover, while treatment with M10T or X-irradiation alone increased mitochondrial ROS production, combined treatment showed no further amplification of this effect (Fig. 5B), suggesting that the M10T-induced increment of mitochondrial ROS production itself does not contribute to its radiosensitization. These results led us to hypothesize that M10T-induced impairment of ATP-dependent cellular survival systems (antioxidant defense, DNA repair, cell cycle checkpoints) triggers inhibition of proliferation, resulting in cell death. As shown in Supplemental Fig. 2, similar results were obtained when using a lower dose of X-irradiation (5 Gy instead of 10 Gy). Furthermore, the correlation between compounds that are radiosensitizing and compounds that abrogate radiation induced upregulation of ATP production also support our hypothesis. Wang and Yi (2008) have proposed a novel strategy of manipulating intracellular ROS or antioxidant levels in chemical and radiation cancer therapy [31]. In this strategy, when both tumor and normal cells are exposed to equal intensities of exogenous ROS-producing or -stimulating agents, intra-cellular ROS levels in tumor cells would sooner reach the threshold to trigger death than those in normal cells. This is because of the higher basal ROS level in tumor cells due either to

increased ROS generation or an impaired antioxidant system. According to this "ROS threshold theory", the radiosensitization mechanism in these experiments may be explained by lipophilic decyl TPP+-mediated reduction in ATP-dependent survival systems in the presence of an apparent increase in harmful ROS. As shown in Figs. 5A and 6, M10T inhibited radiation-induced increases in ATP but not mitochondrial membrane potential. This observation may indicate that M10T predominantly inhibits downstream sites in the ETC such as complex IV or ATP synthase. But, further experiments will be necessary to clarify this radiosensitization mechanism.

In summary, lipophilic decyl TPP^+ derivatives such as M10T, M10T-Me, and M10 enhanced radiation-induced cell death by decreasing intracellular ATP levels, suggesting that the ATP increase response after tumor cells are exposed to ionizing radiation is an adaptive response against oxidative damage as a post-irradiation event. Furthermore, these results indicate that TPP cation conjugated with a long hydrocarbon linker is a candidate novel radiosensitizing agent, targeting radiation-induced activation of mitochondrial ETC in tumor cells.

Acknowledgements

This work was supported, in part, by the JSPS KAKENHI, Japan (No. 25861045 [H.Y.], No. 15K09983 [H.Y.], No. 26461875 [T.Y.] and No. 24659551 [O.I.]) and by the Takeda Science Foundation [H.Y.].

References

[1] O. Warburg, On the origin of cancer cells, Science, 123 (1956) 309-314.
[2] W.X. Zong, J.D. Rabinowitz, E. White, Mitochondria and Cancer, Molecular cell, 61 (2016) 667-676.
[3] X.L. Zu, M. Guppy, Cancer metabolism: facts, fantasy, and fiction, Biochemical and biophysical research communications, 313 (2004) 459-465.
[4] J.K. Leach, G. Van Tuyle, P.S. Lin, R. Schmidt-Ullrich, R.B. Mikkelsen, Ionizing radiation-induced, mitochondria-dependent generation of reactive oxygen/nitrogen, Cancer Res, 61 (2001) 3894-3901.
[5] S.M. Nugent, C.E. Mothersill, C. Seymour, B. McClean, F.M. Lyng, J.E. Murphy, Increased mitochondrial mass in cells with functionally compromised mitochondria after exposure to both direct gamma radiation and bystander factors, Radiat Res, 168 (2007) 134-142.
[6] A. Ogura, S. Oowada, Y. Kon, A. Hirayama, H. Yasui, S. Meike, S. Kobayashi, M. Kuwabara, O. Inanami, Redox regulation in radiation-induced cytochrome c release from mitochondria of human lung carcinoma A549 cells, Cancer Lett, 277 (2009) 64-71.
[7] T. Yamamori, H. Yasui, M. Yamazumi, Y. Wada, Y. Nakamura, H. Nakamura, O. Inanami, Ionizing radiation induces mitochondrial reactive oxygen species production accompanied by upregulation of mitochondrial electron transport chain function and mitochondrial content under control of the cell cycle checkpoint, Free Radic Biol Med, 53 (2012) 260-270.
[8] T. Yamamori, S. Ike, T. Bo, T. Sasagawa, Y. Sakai, M. Suzuki, K. Yamamoto, M. Nagane, H. Yasui, O. Inanami, Inhibition of the mitochondrial fission protein dynamin-related protein 1 (Drp1) impairs mitochondrial fission and mitotic catastrophe after x-irradiation, Molecular biology of the cell, 26 (2015) 4607-4617.
[9] C.L. Lu, L. Qin, H.C. Liu, D. Candas, M. Fan, J.J. Li, Tumor cells switch to mitochondrial oxidative phosphorylation under radiation via mTOR-mediated hexokinase II inhibition--a Warburg-reversing effect, PLoS One, 10 (2015) e0121046.
[10] A.T. Alexandrou, J.J. Li, Cell cycle regulators guide mitochondrial activity in radiation-induced adaptive response, Antioxidants & redox signaling, 20 (2014) 1463-1480.

[11] R.J. Burns, R.A. Smith, M.P. Murphy, Synthesis and characterization of thiobutyltriphenylphosphonium bromide, a novel thiol reagent targeted to the mitochondrial matrix, Arch Biochem Biophys, 322 (1995) 60-68.
[12] T.K. Lin, G. Hughes, A. Muratovska, F.H. Blaikie, P.S. Brookes, V. Darley-Usmar, R.A. Smith, M.P. Murphy, Specific modification of mitochondrial protein thiols in response to oxidative stress: a proteomics approach, J Biol Chem, 277 (2002) 17048-17056.
[13] M. Hardy, F. Chalier, O. Ouari, J.P. Finet, A. Rockenbauer, B. Kalyanaraman, P. Tordo, Mito-DEPMPO synthesized from a novel NH2-reactive DEPMPO spin trap: a new and improved trap for the detection of superoxide, Chem Commun (Camb), (2007) 1083-1085.
[14] Y. Xu, B. Kalyanaraman, Synthesis and ESR studies of a novel cyclic nitrone spin trap attached to a phosphonium group-a suitable trap for mitochondria-generated ROS?, Free Radic Res, 41 (2007) 1-7.
[15] M.P. Murphy, K.S. Echtay, F.H. Blaikie, J. Asin-Cayuela, H.M. Cocheme, K. Green, J.A. Buckingham, E.R. Taylor, F. Hurrell, G. Hughes, S. Miwa, C.E. Cooper, D.A. Svistunenko, R.A. Smith, M.D. Brand, Superoxide activates uncoupling proteins by generating carbon-centered radicals and initiating lipid peroxidation: studies using a mitochondria-targeted spin trap derived from alpha-phenyl-N-tert-butylnitrone, J Biol Chem, 278 (2003) 48534-48545.
[16] K.M. Robinson, M.S. Janes, M. Pehar, J.S. Monette, M.F. Ross, T.M. Hagen, M.P. Murphy, J.S. Beckman, Selective fluorescent imaging of superoxide in vivo using ethidium-based probes, Proc Natl Acad Sci U S A, 103 (2006) 15038-15043.
[17] R.A. Smith, C.M. Porteous, C.V. Coulter, M.P. Murphy, Selective targeting of an antioxidant to mitochondria, Eur J Biochem, 263 (1999) 709-716.
[18] A. Dhanasekaran, S. Kotamraju, C. Karunakaran, S.V. Kalivendi, S. Thomas, J. Joseph, B. Kalyanaraman, Mitochondria superoxide dismutase mimetic inhibits peroxide-induced oxidative damage and apoptosis: role of mitochondrial superoxide, Free Radic Biol Med, 39 (2005) 567-583.
[19] A. Filipovska, G.F. Kelso, S.E. Brown, S.M. Beer, R.A. Smith, M.P. Murphy, Synthesis and characterization of a triphenylphosphonium-conjugated peroxidase mimetic. Insights into the interaction of ebselen with mitochondria, J Biol Chem, 280 (2005) 24113-24126.
[20] M.P. Murphy, R.A. Smith, Targeting antioxidants to mitochondria by conjugation to lipophilic cations, Annu Rev Pharmacol Toxicol, 47 (2007) 629-656.

[21] T.A. Trendeleva, A.G. Rogov, D.A. Cherepanov, E.I. Sukhanova, T.M. Il'yasova, Severina, II, R.A. Zvyagilskaya, Interaction of tetraphenylphosphonium and dodecyltriphenylphosphonium with lipid membranes and mitochondria, Biochemistry (Mosc), 77 (2012) 1021-1028.
[22] T.A. Trendeleva, E.I. Sukhanova, A.G. Rogov, R.A. Zvyagilskaya, Seveina, II, T.M. Ilyasova, D.A. Cherepanov, V.P. Skulachev, Role of charge screening and delocalization for lipophilic cation permeability of model and mitochondrial membranes, Mitochondrion, 13 (2013) 500-506.
[23] J. Trnka, M. Elkalaf, M. Andel, Lipophilic triphenylphosphonium cations inhibit mitochondrial electron transport chain and induce mitochondrial proton leak, PLoS One, 10 (2015) e0121837.
[24] H. Fujimori, A. Sato, S. Kikuhara, J. Wang, T. Hirai, Y. Sasaki, Y. Murakami, R. Okayasu, M. Masutani, A comprehensive analysis of radiosensitization targets; functional inhibition of DNA methyltransferase 3B radiosensitizes by disrupting DNA damage regulation, Scientific reports, 5 (2015) 18231.
[25] A. Ogura, Y. Watanabe, D. Iizuka, H. Yasui, M. Amitani, S. Kobayashi, M. Kuwabara, O. Inanami, Radiation-induced apoptosis of tumor cells is facilitated by inhibition of the interaction between Survivin and Smac/DIABLO, Cancer Lett, 259 (2008) 71-81.
[26] T. Oike, H. Ogiwara, K. Torikai, T. Nakano, J. Yokota, T. Kohno, Garcinol, a histone acetyltransferase inhibitor, radiosensitizes cancer cells by inhibiting non-homologous end joining, International journal of radiation oncology, biology, physics, 84 (2012) 815-821.
[27] I.A. Trounce, Y.L. Kim, A.S. Jun, D.C. Wallace, Assessment of mitochondrial oxidative phosphorylation in patient muscle biopsies, lymphoblasts, and transmitochondrial cell lines, Methods in enzymology, 264 (1996) 484-509.
[28] C. Cottet-Rousselle, X. Ronot, X. Leverve, J.F. Mayol, Cytometric assessment of mitochondria using fluorescent probes, Cytometry A, 79 (2011) 405-425.
[29] J. Montero, M. Mari, A. Colell, A. Morales, G. Basanez, C. Garcia-Ruiz, J.C. Fernandez-Checa, Cholesterol and peroxidized cardiolipin in mitochondrial membrane properties, permeabilization and cell death, Biochimica et biophysica acta, 1797 (2010) 1217-1224.
[30] P. Schonfeld, L. Wojtczak, Fatty acids as modulators of the cellular production of reactive oxygen species, Free Radic Biol Med, 45 (2008) 231-241.
[31] J. Wang, J. Yi, Cancer cell killing via ROS: to increase or decrease, that is the question, Cancer biology & therapy, 7 (2008) 1875-1884.

Figure Legend

Fig. 1.

(A) Chemical structures of lipophilic tetraphenylphosphonium and nitroxide derivatives; Mito-$(CH_2)_{10}$-Tempol (M10T), Mito-$C_{10}H_{21}$ (M10), Mito-$(CH_2)_{10}$-Tempol-Metyl (M10T-Me), $C_{10}H_{21}$-Tempol (10T), and Mito-$(CH_2)_5$-Tempol (M5T). **(B)** Cytotoxicity of the tested compounds in tumor cells. Clonogenic survival of HeLa cells **(a)** and A549 cells **(b)** after treatment with the compounds was assessed by colony formation assay. Tumor cells were treated with M10T (*red closed circles*), M10 (*purple closed triangles*), M10T-Me (*open circles*), 10T (*closed blue diamonds*), and M5T (*closed green squares*) at the indicated concentrations for 12 h.

Fig. 2.

The effects of Mito-tempol derivatives on the mitochondrial membrane potential and the production of ROS from mitochondria. The changes in mitochondrial membrane potential **(A)** and mitochondria-derived ROS **(B)** in HeLa cells after treatment with each compound at 1.5 μM for 12 h. TMRM and MSR were used as fluorescent probes for mitochondrial membrane potential and mitochondria-derived ROS, respectively, and fluorescence intensities were obtained by flow cytometric analysis. The mean fluorescence intensity of each sample was normalized to that of a control sample to calculate the relative fluorescence intensity. Data are expressed as the mean ± S.D. for three experiments. $^{**}p < 0.01$, significant difference vs. control.

Fig. 3

Uptake of Mito-tempol into mitochondria assessed by ESR spectroscopy. **(A)** Mitochondrial (*Mito*), Nuclear (*Nuc*) and cytoplasmic (*Cyto*) fractions were immunoblotted for VDAC1, Lamin B, and GAPDH. In each lane, 7.5 μg of protein was loaded. The Western blots have been performed at least in triplicate, and representative blots are shown. **(B)** Representative ESR spectra derived from M10T **(a)**, M5T **(b)**, and 10T **(c)**, in mitochondrial, nuclear, and cytoplasmic fractions of HeLa cells. Each fractionated sample was oxidized by $K_3Fe(CN)_6$ as described in Materials and Methods. One hundred and ten microliters of each sample was loaded into a quartz flat cell and each ESR spectrum was recorded under the same conditions (receiver gain=100). **(C)** Quantitative data for the uptake of the Mito-tempol compounds. The relative concentrations of nitroxide radicals per 5.5 x 10^6 cells were calculated by double integration of each ESR spectrum and shown as relative values compared with that of M10T in mitochondria. Data are expressed as means ± S.D. for three experiments. *$p < 0.05$, significant difference vs. M10T in each fraction. †$p < 0.05$, significant difference between the fractions in each compound.

Fig. 4.

The radiosensitizing effect of tested compounds in tumor cells. The clonogenic survival of HeLa cells **(A)** and A549 cells **(B)** after treatment with the compounds and X-irradiation were assessed by colony formation assay. Treatment with each compound at concentrations of 1.5 and 0.5 μM was performed for 12 h before X-irradiation of HeLa and A549 cells, respectively. Cells were also exposed to X-rays in the absence of the compounds. Figure symbols are as follows; M10T + X-rays (*red closed circles*),

M10 + X-rays (*purple closed triangles*), M10T-Me + X-rays (*open circles*), 10T + X-rays (*closed blue diamonds*), M5T + X-rays (*closed green squares*), and X-rays alone (*black closed circles*).

Fig. 5.

The effect of combination treatment with M10T and X-irradiation on mitochondrial membrane potential and production of ROS from mitochondria. Twenty-four hours after treatment with M10T (1.5 μM) and subsequent X-irradiation (10 Gy), HeLa cells were collected. **(A)** The post treatment mitochondrial membrane potential of HeLa cells was assessed by TMRM-based flow cytometry. **(B)** The production of ROS from mitochondria was assessed by MSR-based flow cytometry. Data were shown as relative fluorescence intensities normalized to untreated controls. Data are expressed as means ± S.D. for three experiments. *$p < 0.05$, **$p < 0.01$, significant difference vs. no treatment control. ††$p < 0.01$, significant difference vs. M10T alone. N.S., not significant.

Fig. 6.

The effect of combination treatment with Mito-tempol derivatives and X-irradiation on cellular ATP production. Twenty-four hours after treatment with each compound (1.5 μM) and subsequent X-irradiation (10 Gy), HeLa cells were collected. ATP production in cells after treatment was assessed by an ATP-dependent luminescence assay. The data were shown as relative values normalized to untreated controls. Data are expressed as means ± S.D. for three experiments. *$p < 0.05$, **$p < 0.01$, significant difference vs. no irradiation control in each compound. ††$p < 0.01$, significant difference vs. no treatment control. N.S., not significant.

Figure 1
Click here to download high resolution image

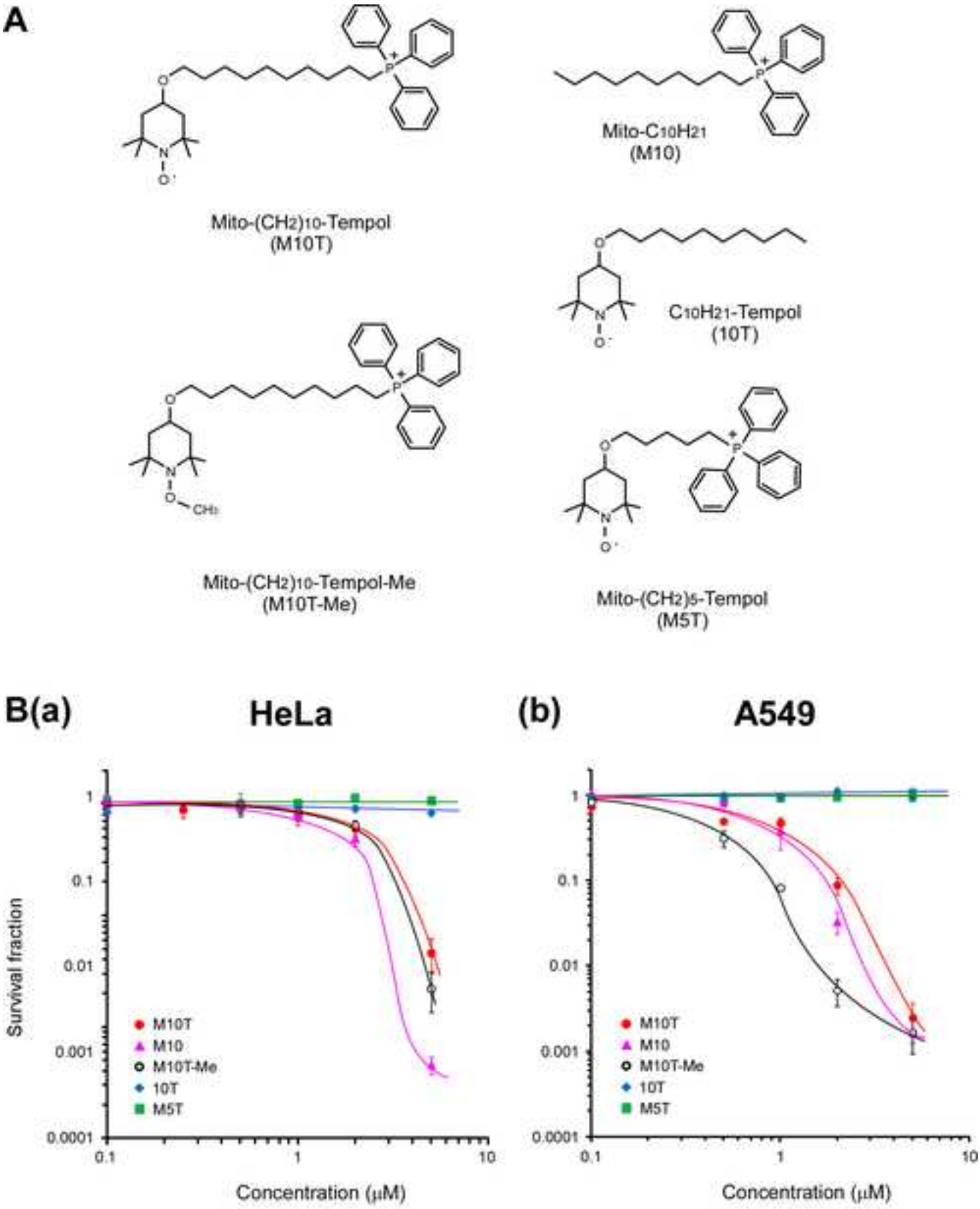

Fig. 1. Yasui et al.

Figure 2
Click here to download high resolution image

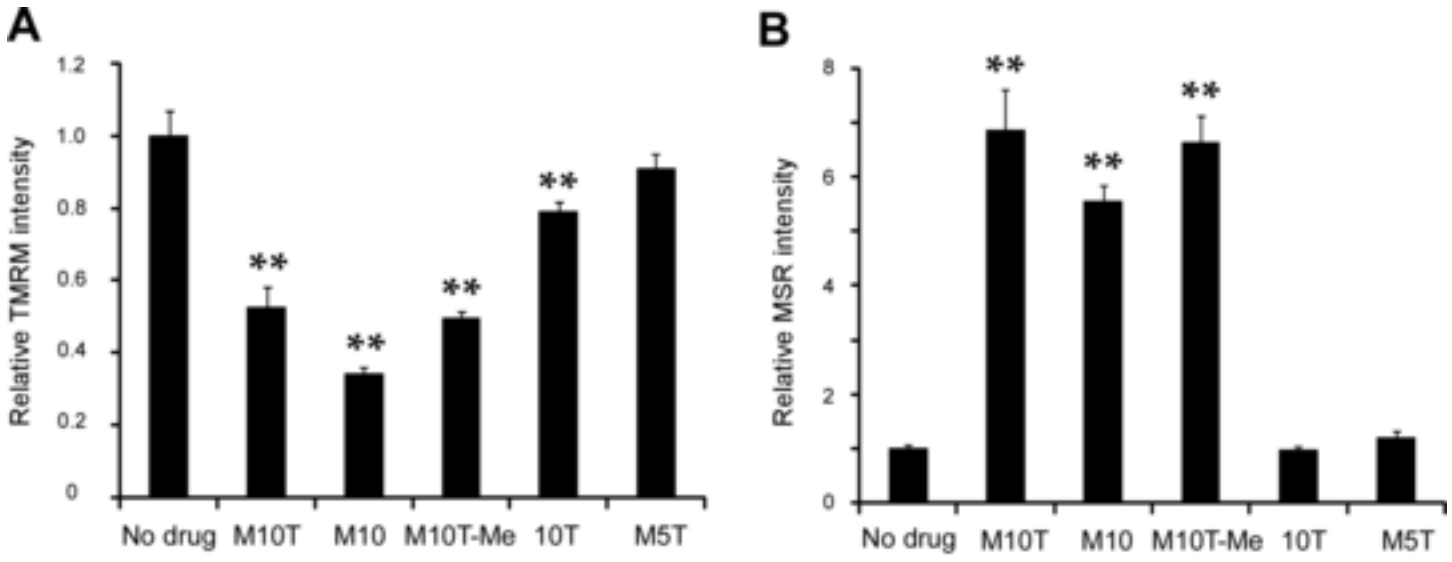

Fig. 2. Yasui et al.

Figure 3
Click here to download high resolution image

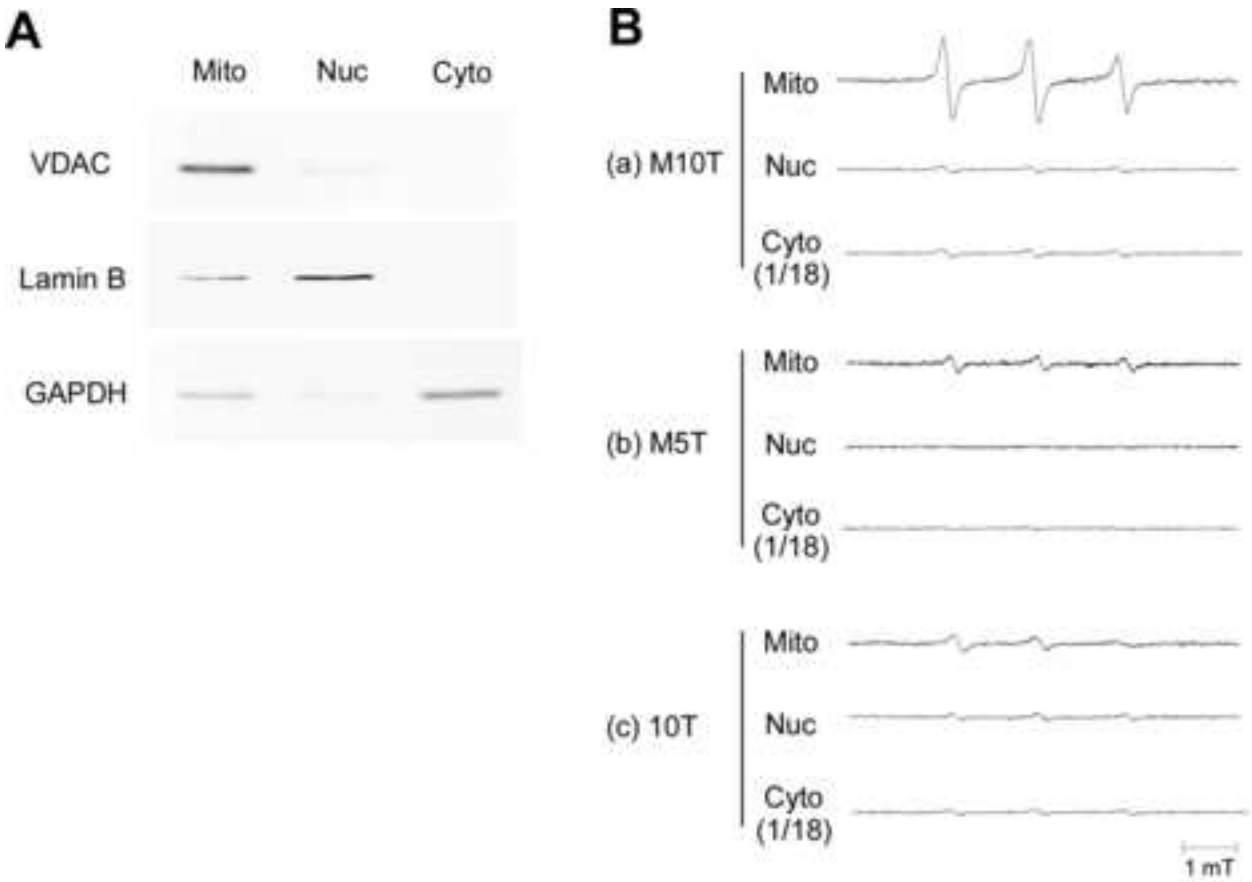

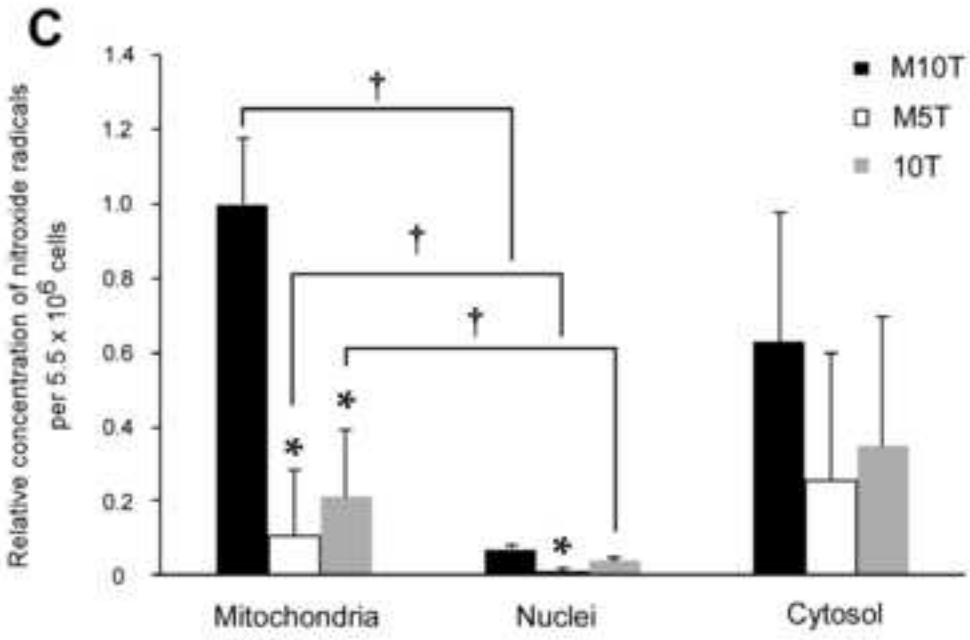

Fig. 3. Yasui et al.

Figure 4
Click here to download high resolution image

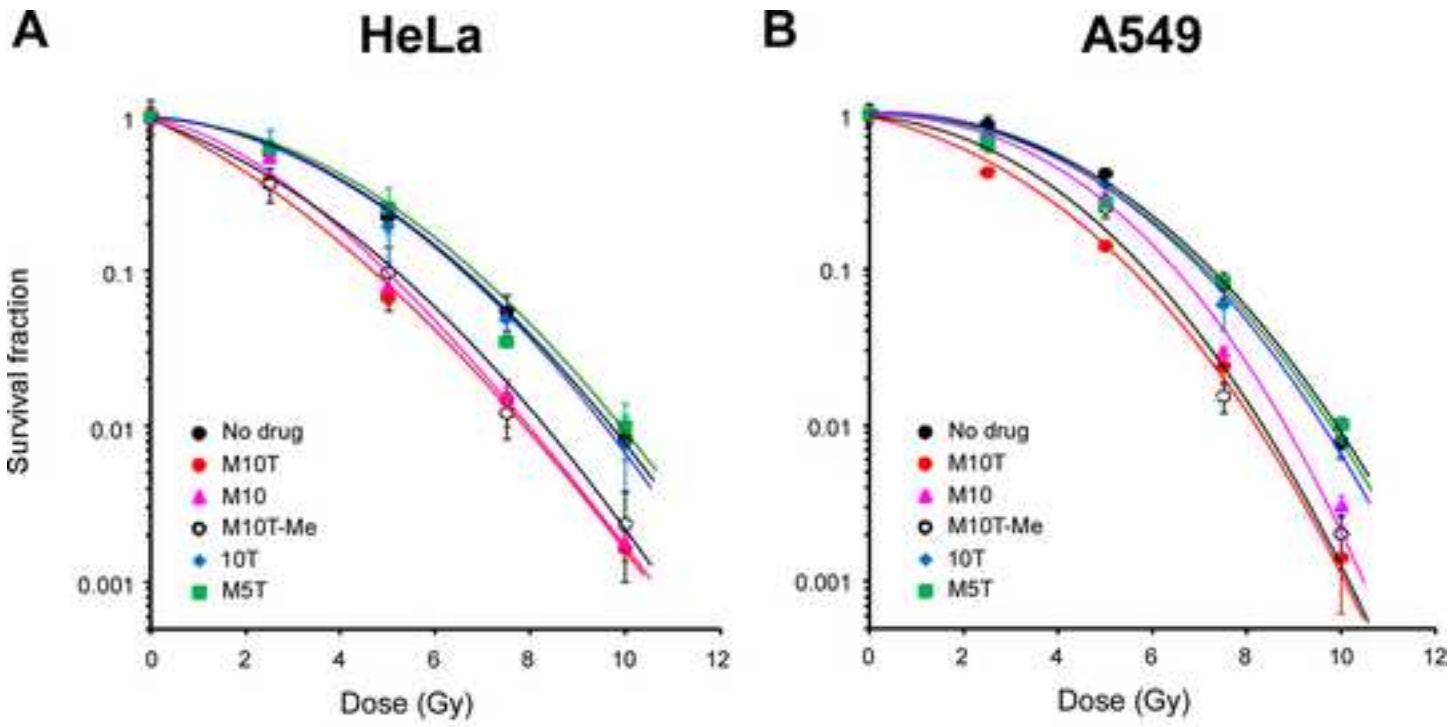

Fig. 4. Yasui et al.

Figure 5
Click here to download high resolution image

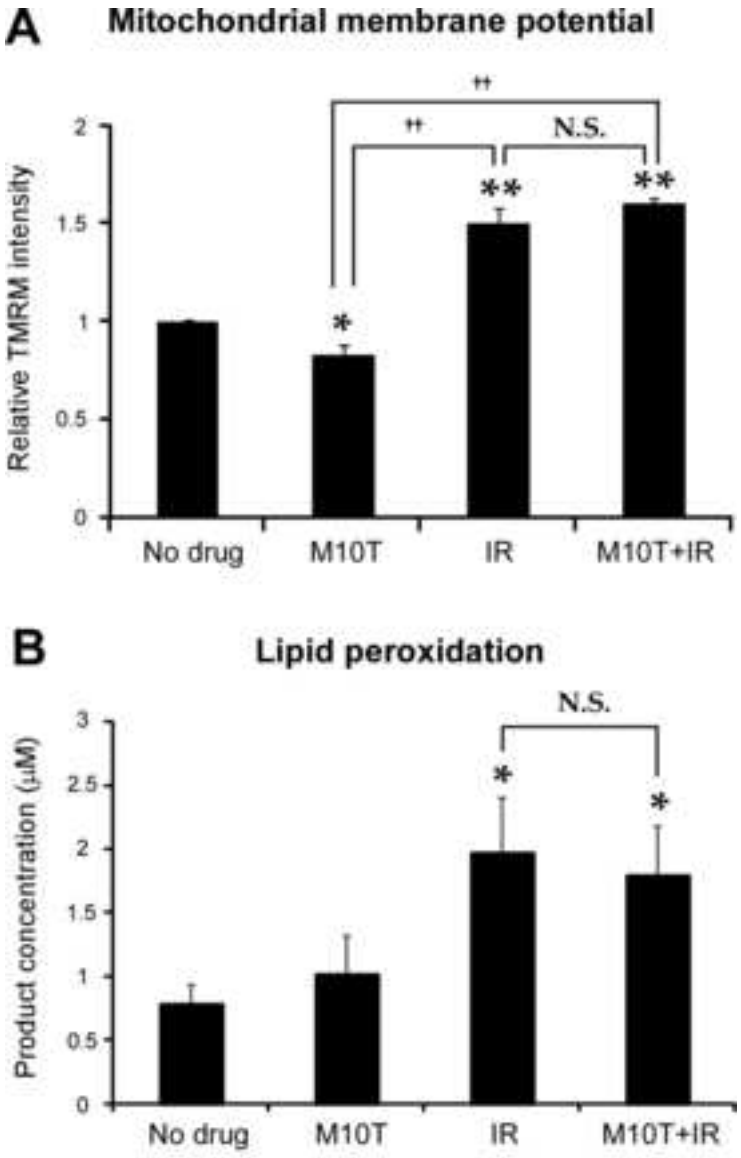

Fig. 5. Yasui et al.

Figure 6

Click here to download high resolution image

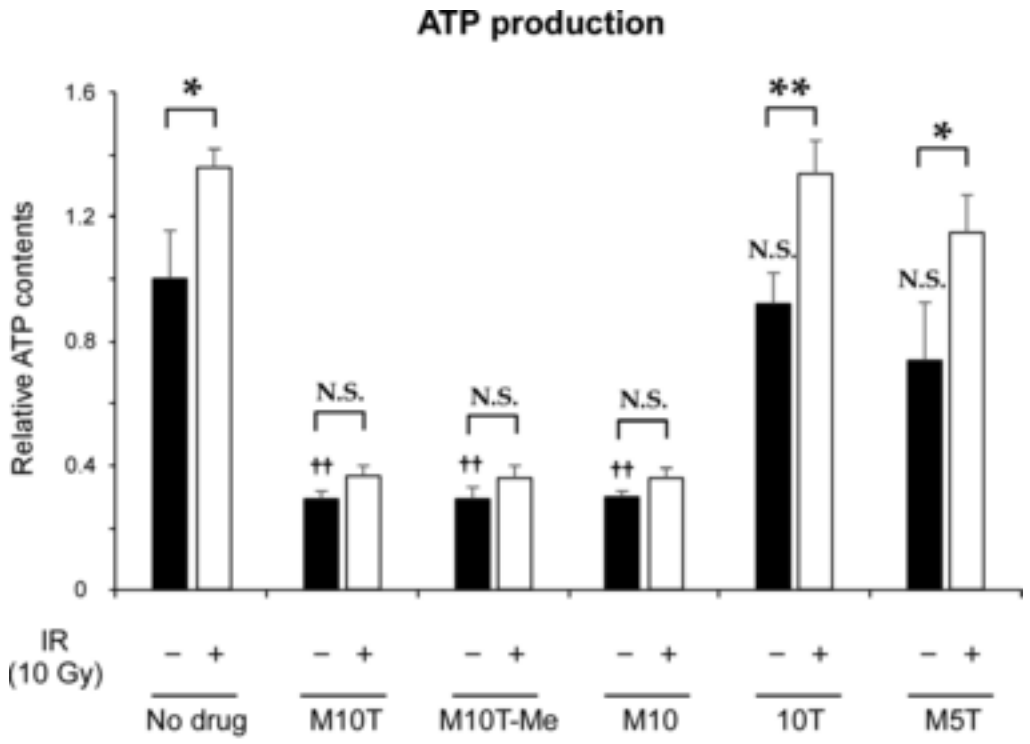

Fig. 6. Yasui et al.

Table 1

Table 1. IC50 of lipophilic TPP^+ derivatives and their related compounds in HeLa and A549 cells

	M10T	M10	M10T-Me	10T	M5T
HeLa	2.33 μM	1.78 μM	2.30 μM	> 5 μM	> 5 μM
A549	0.65 μM	0.80 μM	0.46 μM	> 5 μM	> 5 μM

The IC50 values were calculated based on survival curves using Origin Pro 7 software.

Table 2

Table 2. Survival parameters and sensitizer enhancement ratios for HeLa and A549 cells treated with X-irradiation combining with lipophilic TPP^+ derivatives and their related compounds

	Control	M10T	M10	M10T-Me	10T	M5T
HeLa						
α (Gy^{-1})	0.16	0.35	0.32	0.34	0.16	0.18
SER_{α}		2.18	2	2.13	1	1.25
β (Gy^{-1})	0.03	0.03	0.03	0.03	0.03	0.03
SER_{β}		1	1	1	1	1
D_{10}	6.53	4.58	4.82	4.76	6.41	6.22
SER_{D10}		1.43	1.35	1.37	1.02	1.05
A549						
α (Gy^{-1})	0.01	0.11	0.08	0.07	0.01	0.02
SER_{α}		11	8	7	1	2
β (Gy^{-1})	0.04	0.05	0.05	0.06	0.05	0.05
SER_{β}		1.25	1.25	1.5	1.25	1.25
D_{10}	7.19	5.66	6.15	5.75	7.12	7.19
SER_{D10}		1.27	1.17	1.25	1.01	1

The biological parameters and sensitizer enhancement ratios (SER) were calculated based on survival curves. Calculation formula is shown in Materials and Methods.